MOLECULAR IMAGING AND BIOLOGY

Published Online: 10 November 2007

Mol Imaging Biol (2008) 10:54–61
DOI: 10.1007/s11307-007-0120-5

RESEARCH ARTICLE

Noninvasive Real-time Imaging of Tumors and Metastases Using Tumor-targeting Light-emitting *Escherichia coli*

Jung-Joon Min,[1] Hyun-Ju Kim,[2] Jae Hyo Park,[1] Sungmin Moon,[1] Jae Ho Jeong,[2] Yeoung-Jin Hong,[2] Kyoung-Oh Cho,[3] Jong Hee Nam,[4] Nacksung Kim,[5] Young-Kyu Park,[6] Hee-Seung Bom,[1] Joon Haeng Rhee,[2] Hyon E. Choy[2]

[1]*Laboratory of In Vivo Molecular Imaging, Department of Nuclear Medicine, Chonnam National University Medical School, Gwangju, South Korea*
[2]*Department of Microbiology, Chonnam National University Medical School, Gwangju, South Korea*
[3]*Department of Pathology, Chonnam National University College of Veterinary Medicine, Gwangju, South Korea*
[4]*Department of Pathology, Chonnam National University Medical School, Gwangju, South Korea*
[5]*Department of Pharmacology, Chonnam National University Medical School, Gwangju, South Korea*
[6]*Department of Surgery, Chonnam National University Medical School, Gwangju, South Korea*

Abstract

Purpose: A number of bacteria types are known to preferentially grow in tumors. We have taken advantage of this phenomenon to target luciferase-expressing *Escherichia coli* to tumors and metastases in mouse models to image them noninvasively.

Methods and Results: After intravenous injection of pLux-expressing *E. coli* (10^8 CFU), bioluminescence signals from the bacteria were detected exclusively in tumor tissue after 24 hours. The balanced-lethal host–vector system using the gene encoding aspartate β-semi-aldehyde dehydrogenase (*asd*) enabled stable maintenance of the pLux in the tumor-targeting *E. coli*. This phenomenon of selective tumor targeting and proliferation of *E. coli* was observed in a diverse range of tumors implanted in nude mice. More importantly, *E. coli* was capable of targeting both primary tumors and metastases, enabling them to be imaged noninvasively in both nude and immunocompetent mice.

Conclusions: Our results suggest the potential clinical use of this technology for tumor targeting.

Key words: Tumor imaging, Noninvasive small animal imaging, *Escherichia coli*, Bacterial luciferase (Lux), Green fluorescent protein (GFP), Cancer-targeting bacteria

Introduction

For the last several decades, a number of microorganisms have been shown to display selective replication or preferential accumulation in tumor [1, 2]. This feature has been exploited to treat cancer directly or in combination with conventional chemotherapy [3]. Early observations demonstrated that certain anaerobic *Clostridium* species could proliferate extensively in the hypoxic and necrotic regions of some tumors, whereas they would not grow in well-oxygenated normal tissues [1, 4–6]. Recently, Vogelstein and coworkers created an anaerobic strain of *Clostridium novyi* in which the lethal toxin was removed. After intravenous administration into mice, its spores germinated within the avascular regions of tumors, destroying the surrounding viable tumor cells [7]. However, facultative anaerobes such as *Escherichia coli* and *Salmonella* spp. also localize to transplanted tumors in animals

Correspondence to: Jung-Joon Min; *e-mail:* jjmin@jnu.ac.kr

and can grow in viable as well as necrotic areas of the tumor, which are potential important advantages [2, 8–12]. According to the most current publication by Hoffman and coworkers, weekly treatment with attenuated *Salmonella typhimurium* resulted in the inhibition of tumor growth and metastasis for a long period and eventual cures [13]. Thus, although the mechanism underlying the initial accumulation or tumor destruction remains to be understood, attempts have been made to treat tumors using various microorganisms.

Light-emitting microorganisms including *E. coli*, *Salmonella typhimurium*, *Vibrio cholerae*, and *Listeria monocytogenes* expressing luciferase (Lux) or green fluorescence protein (GFP) have been used to target and visualize tumors in mouse models [2, 14]. These studies, however, raised the following questions: (1) could the less virulent *E. coli* be used as a molecular imaging probe or a drug delivery vector in different tumor models?; (2) could this phenomenon provide a reliable and noninvasive whole-body imaging method that could be interpreted clearly?; and (3) could *E. coli* maintain a stable light signal in the absence of external selection, thus rendering it appropriate for *in vivo* preclinical imaging and potential clinical use?

In this study, we constructed a light-generating strain of *E. coli* expressing pLux that could be stably imaged in mouse models over extended periods. Most importantly, the *E. coli* accumulated selectively in tumors and metastases enabling them to be imaged noninvasively.

Materials and Methods

Bacterial Strains and Plasmids

Table 1 lists the *E. coli* strains (MG1655 and HJ1020) and plasmids used for this study. Bacterial strains were constructed using P1 transduction, as described previously [15]. The *E. coli asd*::*kan* strain (HJ1020) was constructed from MG1655 by linear DNA transformation method as described previously [16]. PCR amplification of pKD13 was used to replace the *asd* open reading frame (ORF) with *kan*. The primers were as follows: forward, 5′-CACTTGCGACTTTGGCTGCTTTTTGTATGGTGAAAGATGTGCCAAGAGGAGACCGGCACATTTATACAGCACGTGTAGGCTGGAGCTGCTTC-3′ and reverse, 5′-CCCTTAAAGAATAGCCAATGCTCTATTTAACTCCCGGTAAATCATGAAACATCTGCGCTTACTCCTGTATTACGCTTCCGGGGATCCGCTGACC-3′. *kan* was then removed, generating Δ*asd* according to the method described by Datsenko and Wanner [16].

Table 1. *E. coli* strains and plasmids

Strains/plasmids	Description	Reference/source
MG1655	Wild type	
HJ1020	Δ*asd*	This work
pLux	pUC19 with *luxCDABE*	This work; [17]
Asd$^+$ pLux	pLux with the *asd* ORF	This work; [18]
pEGFP	pUC19 with *gfp*	Clontech (USA)

The luminescence-expressing plasmid pLux was constructed by ligating a 9.5-kb *Xba*I fragment from pT7-3-Lux (which contained *luxCDABE* from *Photobacterium leiognathi* [17] into the same site in pUC19 where the *lux* operon could be driven by the *lac* promoter). To construct a plasmid containing both the *lux* cassette and *asd* [18], we PCR-amplified the *asd* gene from *E. coli* (MG1655) genomic DNA using the primers ASD1 (5′-CGCGCAGGGCCCGCACATCTCTTTGCAGGAAAA-3′) and ASD2 (5′-CTGCAAGCATGCCTACGCCAACTGGCGCAGCAT-3′). This 1.1-kb fragment was cloned into pGEM-T Easy (Promega, Madison, WI, USA), digested with *Eco*RI, and ligated into the same site in pLux, generating the construct Asd$^+$ pLux. pEGFP was purchased from Clontech (Mountain View, CA, USA).

Cell Lines

The CT26 mouse colon adenocarcinoma cell line, C6 rat glioma cell line, and the 4T1 and 4TO7 mouse breast cancer cell lines [19] were grown in high-glucose Dulbecco's modified Eagle medium (DMEM) containing 10% FBS and 1% penicillin–streptomycin. The SNU-C5 human colon adenocarcinoma cell line [20] and B16F10 mouse melanoma cell line [21] were grown in RPMI 1640 containing 10% FBS and 1% penicillin–streptomycin.

Animal Models

Five- to six-week-old male BALB/c and BALB/c athymic nu^-/nu^- mice (20–30 g body weight) were purchased from the Shizuoka Lab Animal Center (SLC), Japan. All animal care, experiments, and euthanasia were performed in accordance with protocols approved by the Chonnam National University Animal Research Committee. Anesthesia of animals was performed using isoflurane (2%) during imaging or a mixture of ketamine (200 mg kg^{-1}) and xylasine (10 mg kg^{-1}) for surgery.

Nude mice carrying subcutaneous tumors were generated as follows: CT26, C6, SNU-C5, and B16F10 cells were harvested, after which 10^6 cells were suspended in 100 µl PBS and injected subcutaneously into either the thigh or right shoulder of each mouse. Tumor volume (mm^3) was estimated using the formula $(L\times H\times W)/2$ where L is the length, W is the width, and H is the height of the tumor in millimeters [2].

We used nude mice bearing subcutaneous CT26 tumors to generate orthotopic intracolonic adenocarcinoma models. When the subcutaneous tumor volume reached 500 mm^3, fresh tissue was harvested from the periphery of the mass and minced into 1.5-mm^3 fragments. Nude mice were anesthetized by a mixture of ketamine and xylasine, then the abdomen was sterilized and a small vertical incision was made in the left upper quadrant. The colocecal portion of the colon was exteriorized and a pocket introduced into the cecum using a seromuscular purse-string suture (7-0 nylon suture material). A tumor fragment was then implanted into the pocket, the intestine returned to the abdominal cavity, and the abdomen closed using 6-0 surgical sutures [22].

Metastatic tumor models were generated by subcutaneous injection of 10^6 4T1 murine breast cancer cells (which metastasize to the liver and lung) into the fourth mammary fat pad of BALB/c mice.

Injection of Bacteria into Animals

Light-emitting *E. coli* (1×10^8), suspended in 100 µl PBS, were injected intravenously or intraperitoneally into tumor-bearing mice through the lateral tail vein using a 1-cc insulin syringe.

Table 2. Quantification of *E. coli* Asd^+ pLux in various organs and grafted tumors after i.v. injection of CT26 colon cancer into mice

	20 minutes	Four hours	Day 1	Day 2	Day 4	Day 6	Day 8
Tumor	9.52×10^2 ±3.18	1.54×10^3 ±2.21	5.11×10^6 ±2.83	8.96×10^7 ±2.54	3.53×10^8 ±3.57	5.62×10^8 ±4.61	6.85×10^8 ±2.86
Liver	7.10×10^6 ±1.68	2.24×10^6 ±0.78	5.48×10^3 ±0.45	1.40×10^2 ±0.60	0	0	0
Spleen	1.60×10^7 ±0.24	1.52×10^6 ±0.79	1.12×10^3 ±0.62	8.15×10^1 ±3.84	0	0	0
Lung	2.00×10^4 ±0.23	1.13×10^3 ±0.93	0	0	0	0	0

Each organ was removed aseptically at the times indicated. Organs were weighed, homogenized, and plated onto LB agar containing ampicillin (50 μg ml^{-1}). Plates were incubated overnight at 37°C, after which colonies were counted and CFU g^{-1} tissue calculated.

Quantification of E. coli Accumulation

At the times specified in Table 2, animals were euthanized and placed in 70% ethanol for three minutes. Tissues were removed, placed individually into sterile tubes containing PBS at 4°C, and weighed. Samples were then transferred to sterile homogenization tubes where they were homogenized then returned to their original tubes for serial dilution with PBS. Agar plates containing ampicillin (50 μg ml^{-1}) were inoculated with diluted homogenate and incubated overnight at 37°C. Colonies were enumerated and bacterial loads expressed as CFU g^{-1} tissue.

Histology

Mice were euthanized via ethyl ether inhalation. Tumor samples were obtained from experimental mice injected with bacteria-expressing GFP [9]. For histology and direct detection of bacteria, a portion of the tumor tissue was fixed in 10% neutral buffered formalin, processed for paraffin embedment, sectioned, and stained with hematoxylin and eosin (H&E). In addition, sections were Gram stained. To evaluate the localization of GFP-expressing bacteria, a frozen section was obtained from a part of the sample. This was fixed with cold acetone and double-stained with Texas Red-X phalloidin (Invitrogen, Carlsbad, CA, USA) and 4′,6-diamidine-2-phenylindole hydrochloride, which stain F actin in the cytoplasm and nuclei, respectively. Stained samples were mounted using the SlowFade® Antifade Kit (Invitrogen, Carlsbad, CA, USA). Slides were examined using a confocal microscope (Radiance 2100, Bio-Rad, London, UK) equipped with a green helium/neon (543 nm) laser, blue laser diode (405 nm), and red laser diode (637 nm). The resulting images were analyzed using an image-merging program (LaserSharp2000 software, Bio-Rad, London, UK).

Optical Imaging Using a Cooled Charged Couple Detector Camera System

To image bacterial bioluminescence, anesthetized animals were placed in the light-tight chamber of the IVIS100 (Caliper, Hopkinton, MA, USA), equipped with a cooled charged couple detector (CCD) camera. Photons emitted from luciferase-expressing bacteria were collected and integrated over one-minute periods. Pseudocolor images indicating photon counts were overlaid on photographs of the mice using the Living Image software v. 2.25 (Caliper, Hopkinton, MA). A region of interest (ROI) was selected manually over the signal intensity. The area of the ROI was kept constant, and the intensity was recorded as maximum (photons·s^{-1}·cm^{-2}·sr^{-1}[steradian]) within an ROI.

Results

Minimum Number of E. coli Needed for Noninvasive Imaging

Various quantities of *E. coli* were injected subcutaneously into nude mice and the bioluminescence signals determined (Fig. 1). We observed that the minimum number of *E. coli* required for imaging was approximately 10^4 and that

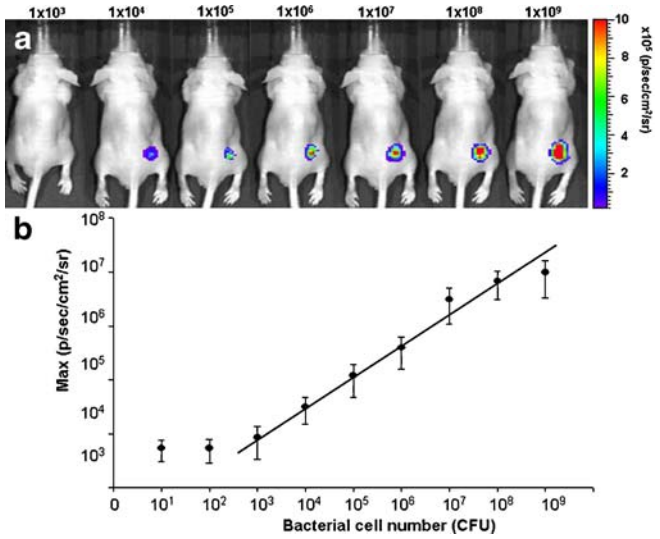

Fig. 1. Minimum number of *E. coli* pLux required for detecting photons. **a** Different quantities of *E. coli* pLux (10^3 to 10^9 CFU) were injected subcutaneously into mice, and the bioluminescence signal determined. The *Y*-axis indicates photons × 10^5·s^{-1}·cm^{-2}·sr^{-1}. **b** The ROI was selected manually for quantification of photon flux. The ROI area was kept constant, and the intensity was recorded as a maximum (photons·s^{-1}·cm^{-2}·sr^{-1}) within the ROI. The photon intensity was plotted as a function of bacterial cell number (CFU). The means and SEM were determined from three independent experiments.

at $\leq 10^9$ CFU, the intensity of bioluminescence correlated directly with the number of bacteria. Thus, the spatial and temporal progression of light-emitting *E. coli* should be traceable in live animals as long as $>10^4$ CFU are present at a specific locus.

Tumor Targeting of Light-Emitting E. coli

We determined the biodistribution of *E. coli* expressing *lux* using mice tumor models. In the absence of selection, it was virtually impossible for *E. coli* to maintain the plasmid, especially in the infected animal (see below). Therefore, we employed a balanced-lethal host–vector system using the gene-encoding aspartate β-semialdehyde dehydrogenase (*asd*). *E. coli asd* mutants have an obligate requirement for diaminopimelic acid (DAP) and undergo lysis in its absence. To retain plasmids *in vivo*, the chromosomal copy of *asd* was mutated in the host strain and complemented by the Asd^+ pLux construct [18, 23, 24].

We then determined the spatial distribution of *E. coli* carrying either pLux (Fig. 2a) or Asd^+ pLux (Fig. 2b), using nude mice ($n>6$) in which the CT26 mouse colon cancer had been implanted in the right lateral thigh 14 days before infection. *E. coli* (10^8 CFU) was injected intravenously into each mouse via the tail vein. Whole-body images were then collected. During the first few hours, bioluminescence signals were detected mainly in the spleen and liver of these mice. However, the signals from both plasmids diminished in the liver from day 1 and signals were eventually detected exclusively in the tumor region.

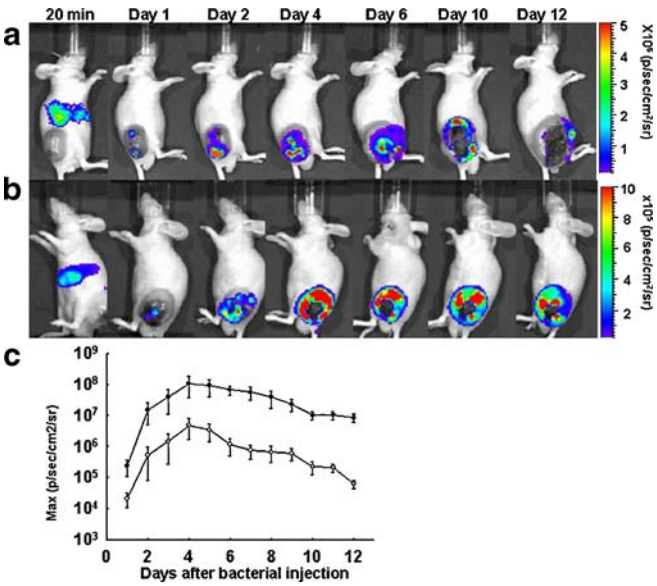

Fig. 2. Distribution of *E. coli* carrying either pLux or Asd^+ pLux in nude mice with orthotopic CT26 colon cancer. *In vivo* bioluminescence imaging was performed on a nude mouse with CT26 mouse colon cancer in the right lateral thigh. 1×10^8 *E. coli* MG1655 pLux (**a**) or *E. coli* HJ1020 Asd^+ pLux (**b**) were injected intravenously via the tail vein. The *Y*-axis indicates photons $\times 10^5 \cdot s^{-1} \cdot cm^{-2} \cdot sr^{-1}$. **c** Photon intensity in the tumor region was plotted as a function of time for *E. coli* pLux (*open circles*) or Asd^+ pLux (*closed circles*). The ROI was selected manually over the tumor region, and the area was kept constant. Photon intensity was recorded as a maximum (photons$\cdot s^{-1} \cdot cm^{-2} \cdot sr^{-1}$) within a ROI. The means and SEM were determined from three independent experiments.

In the tumor tissue, quantified photon flux was plotted as a function of time and we observed that it was approximately tenfold higher for *E. coli* carrying Asd^+ pLux than pLux alone (Fig. 2c). Continued monitoring revealed that for *E. coli* pLux, light emission in the tumor peaked at 4 days post inoculum (dpi) and decreased thereafter to undetectable levels, whereas emission levels were maintained for *E. coli* Asd^+ pLux. It is likely that plasmid loss was responsible for the decrease in bioluminescence emitting from *E. coli* pLux. In contrast, the balanced-lethal host–vector system based on Asd allowed us to continue to monitor the bacteria in the absence of selection pressure for extended period of time, up to 20 days (data not shown).

To correlate imaging and bacterial growth in tumors and normal organs, we determined the actual bacterial number after the injection of *E. coli* Asd^+ pLux. Immediately after injection (20 minutes), the highest bacterial loads were observed in the spleen (1.6×10^7 g^{-1}), liver (7.1×10^6 g^{-1}), and lung (2.0×10^4 g^{-1}), whereas the bacteria present in the tumor (9.5×10^2 g^{-1}) remained at relatively low levels (Table 2). Within 24 hours, the number of bacteria in the tumor tissue increased dramatically (>1,000-fold), reaching approximately 10^8 CFU g^{-1} in 4 dpi. These bacterial titers in the tumors were maintained for the duration of the experiment, whereas those of the liver, spleen, and lung declined and were undetectable after 4 dpi. These results suggest that in internal organs the bacteria were cleared rapidly, whereas in the tumor tissue the bacteria not only survived but proliferated dramatically.

It should be noted that although the light-generating *E. coli* bacteria were detected initially towards the center of the tumor, as the infection progressed they appeared to spread to the border between the necrotic and viable areas of the tumor. To analyze bacterial distribution in the tumor masses, we performed an intravenous injection of *E. coli* (10^8) Asd^+ pLux into nude mice with orthotopic CT26 colon cancer and removed the tumor for cross-sectional analysis at 7 dpi. In the sequentially cross-sectioned tumor mass, necrotic tissue could be distinguished easily from healthy tissue by color, i.e., the central necrotic region was gray, whereas the peripheral proliferative region was pink (Fig. 3a). In addition, we observed strong luciferase-based light emission in the central necrotic region but not at the periphery (Fig. 3b).

Subsequently, we performed a confocal microscopic analysis on tumor tissue obtained from mice infected with *E. coli* pGFP and observed that GFP-expressing bacteria could be visualized by both H&E and Gram staining (Fig. 3c), as well as by fluorescence (Fig. 3d). Bacteria were found in the border region between the peripheral proliferative and central

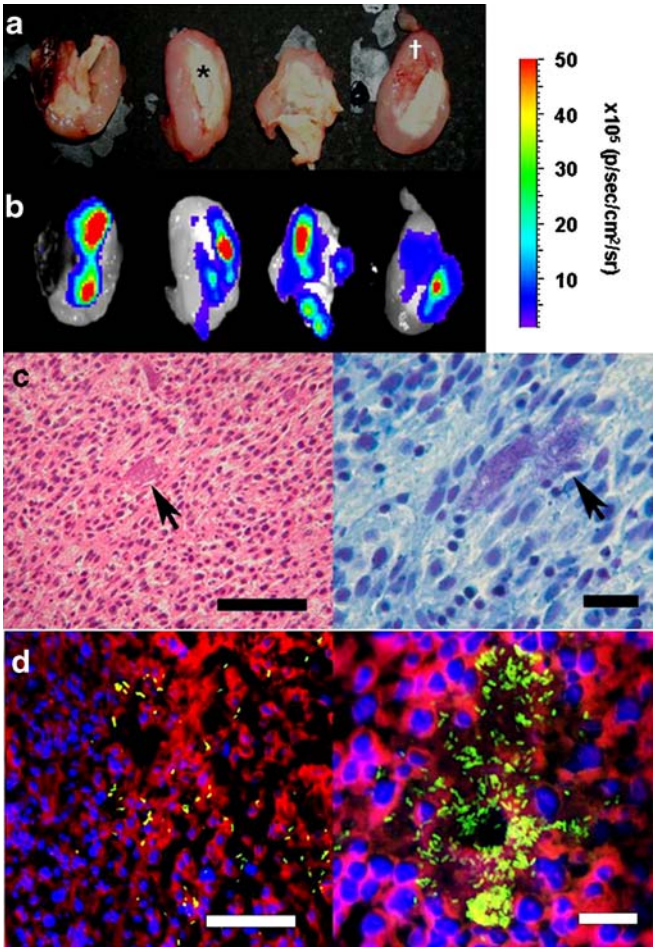

Fig. 3. Distribution of *E. coli* in tumor tissues. **a** and **b** Cross sections of grafted CT26 colon cancer from nude mice after injection of *E. coli* Asd$^+$ pLux were made at 7 dpi. **a** and **b** Show cooled CCD bright field and bioluminescence images from the same cross section, respectively. The *Y*-axis indicates photons $\times 10^5 \cdot s^{-1} \cdot cm^{-2} \cdot sr^{-1}$. In **a**, the central necrotic and peripheral proliferative areas are marked with an *asterisk* and a *cross*, respectively. **c** and **d** Microscopic localization of *E. coli* pGFP in tumor tissue (see the "Materials and Methods" section). **c** Bacterial colonies were stained and visualized in subcutaneous CT26 tumor. *Left*, hematoxylin and eosin (H&E) staining at $\times$200 magnification (bar = 150 μm). *Right*, Gram staining at $\times$400 magnification (bar = 50 μm). *Arrows* indicate bacterial colonies. **d** GFP-expressing *E. coli* (*green*) were visualized under confocal microscopy after staining with Texas red (actin, *red*) and DAPI (nuclei, *blue*). *Left*, $\times$600 magnification (bar = 60 μm). *Right*, $\times$1,200 magnification (bar = 20 μm).

necrotic regions, but were not observed in the peripheral proliferative region of the tumor. These results may suggest that intravenously injected bacteria reach the central necrotic region of the tumor [25–27], subsequently spreading to the border region where they might have induced additional tumor necrosis. Consistently, we observed more tumor necrosis in infected mice than in uninfected mice (data not shown).

Imaging Primary Tumors Using Luciferase-expressing E. coli

We then examined the types of tumors that could be imaged successfully with *E. coli* (Fig. 4). To determine whether we could observe bacterial accumulation in small tumors, nude

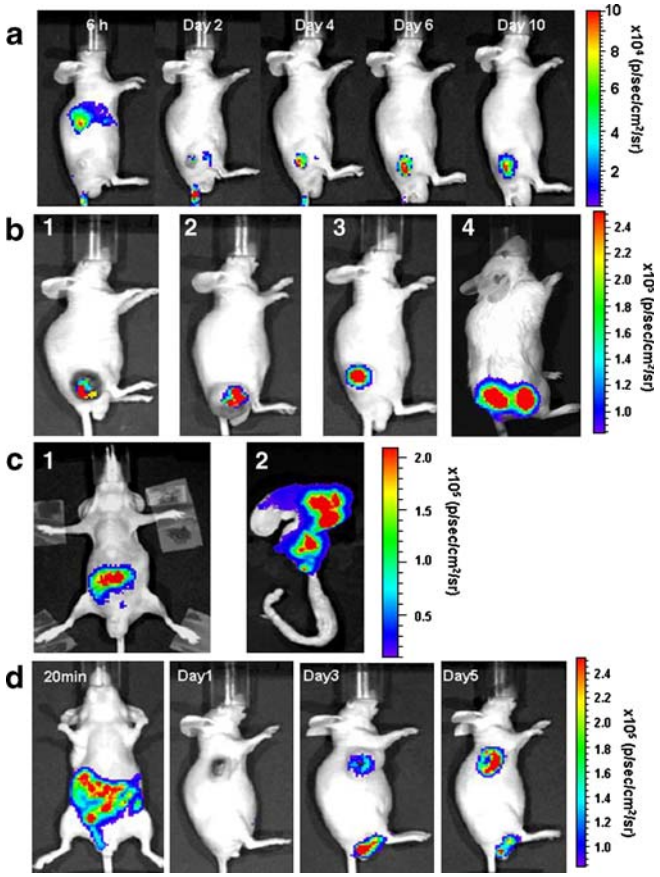

Fig. 4. Visualization of various tumor types using luciferase-expressing *E. coli*. **a** *E. coli* Asd$^+$ pLux cells were injected intravenously into nude mice with CT26 tumors of approximately 50 mm^3. Whole-body photon counting was performed for 1 min. (**b**) Nude mice ($n = 6$) carrying B16F10 mouse melanoma (*1*), C6 rat glioma (*2*), or SNU-C5 human colon cancer (*3*) in the right lateral thigh received intravenous injections of 10^8 *E. coli* (HJ1020) Asd$^+$ pLux. Immunocompetent BALB/c mice ($n = 6$) with subcutaneous orthotopic CT26 tumors received *E. coli* (HJ1020) Asd$^+$ pLux, as described above (*4*). Whole-body photon counting with a cooled CCD camera was performed at 7 dpi. The *Y*-axis indicates photons $\times 10^5 \cdot s^{-1} \cdot cm^{-2} \cdot sr^{-1}$. **c** A nude mouse carrying an intracecal adenocarcinoma was injected intravenously with 10^8 *E. coli* Asd$^+$ pLux cells and whole-body photon counting was performed at 7 dpi (*1*). The mouse was killed on the same day (7 dpi), the intestinal tract excised, and photon counting performed (*2*). The *Y*-axis indicates photons $\times 10^5 \cdot s^{-1} \cdot cm^{-2} \cdot sr^{-1}$. **d** *E. coli* Asd$^+$ pLux cells were injected intraperitoneally into nude mice carrying CT26 tumors on the right shoulder. Photon counting was performed for one minute. The *Y*-axis indicates photons $\times 10^5 \cdot s^{-1} \cdot cm^{-2} \cdot sr^{-1}$.

mice bearing CT26 tumors (approximately 50 mm^3) were injected intravenously with *E. coli* Asd^+ pLux. We observed bioluminescence signal from day 2 when the tumor size reached 100 mm^3, indicating that these bacteria are capable of colonizing small tumors (Fig. 4a). In the subsequent experiment, subcutaneous tumor models were generated with a variety of tumor cell lines: murine melanoma B16F10 (Fig. 4b, 1); rat glioma C6 (Fig. 4b, 2); and human colon cancer SNU-C5 (Fig. 4b, 3). In addition, an orthotopic syngeneic tumor model was generated with CT26 in immunocompetent BALB/c mice. *E. coli* Asd^+ pLux was injected intravenously into each of these tumor-bearing nude and immunocompetent mice, and whole-body bioluminescence images revealed selective accumulation and replication of bacteria in the tumors (Fig. 4b, 4). Notably, *E. coli* was able to colonize tumors in immunocompetent mice.

Next, we investigated bacterial imaging of intracecal adenocarcinomas generated via cecal implantation of peripheral tumor fragments from subcutaneously implanted CT26 tumors (Fig. 4c). Seven days after intracecal implantation, nude mice received an intravenous injection of *E. coli* Asd^+ pLux via the tail vein. Whole-body bioluminescence images were collected at 7 dpi, and a bioluminescence signal was detected in the colocecal area (Fig. 4c, 1). Using the cooled CCD camera, we examined the excised intestinal tract and observed strong bioluminescence at the implanted tumor site (cecal area); no bioluminescence was detected in the normal intestinal tract tissue (Fig. 4c, 2). These results indicate that *E. coli* selectively targets and replicates in colon cancers generated intracecally, as well as in a variety of tumors grafted subcutaneously.

In addition, we investigated whether *E. coli* Asd^+ pLux (10^8) injected intraperitoneally could target subcutaneous CT26 tumors generated in the right shoulder of nude mice. Initially, we observed a diffuse bioluminescence signal in the peritoneal cavity, which disappeared by 1 dpi; by day 3, the signal was detected exclusively in the tumor (Fig. 4d). This indicates that bacteria injected intraperitoneally entered the blood stream and reached the tumors in a similar manner to those injected intravenously.

Imaging Metastases Using Luciferase-expressing E. coli

In addition, we established a hepatic metastatic model using the 4T1 murine breast cancer cell line, which metastasizes to the liver and lung [19]. As a negative control, we employed the murine breast cancer cell line 4TO7, which produces tumors but fails to metastasize [19]. Breast cancer cells (10^6) were injected directly into the right fourth mammary fat pad of BALB/c mice to establish an orthotopic breast cancer and metastasis. After one month, *E. coli* Asd^+ pLux was injected intravenously and the bioluminescence signal traced for three days using a cooled CCD camera (Fig. 5a and b). Immediately after injection (20 minutes), bacterial bioluminescence was confined to the liver region, as observed previously. In both types of tumor, bacterial bioluminescence was detected at the primary tumor site (abdominal mammary fat pad) by 2 dpi. However, only mice carrying the metastatic 4T1 tumor cells exhibited continuing bioluminescence in the liver region, indicating the presence of metastases in this organ. Histological observation confirmed the presence of metastatic murine cancer lesions (Fig. 5c) and bacterial colonies (Fig. 5d) in the bioluminescence-positive livers of mice that received 4T1 cells, whereas no lesions and bacterial colonies were observed in the bioluminescence-negative livers of those that received 4TO7 cells (Fig. 5e). Thus, *E. coli* is capable of targeting both primary tumors and metastases and enables noninvasive imaging of both.

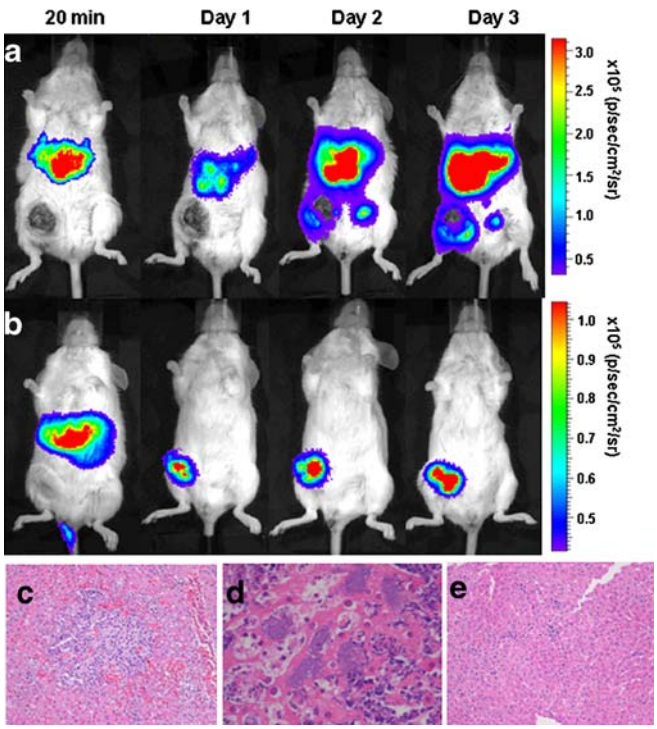

Fig. 5. Bacterial localization in metastatic lesions. **a** Highly metastatic 4T1 murine breast cancer cells were implanted in the abdominal mammary fat pad of a BALB/c mouse. *E. coli* (HJ1020) Asd^+ pLux cells (10^8) were injected intravenously and whole-body photon counting was performed daily. The animal was placed in a supine position and photons were counted for one minute. **b** Whole-body bioluminescence image of a BALB/c mouse implanted with the nonmetastatic 4TO7 murine breast cancer cells and treated as described above. The *Y*-axis indicates photons $\times 10^5 \cdot s^{-1} \cdot cm^{-2} \cdot sr^{-1}$. Animals were killed at 3 dpi and hepatic tissues were examined histologically using H&E staining on **c**–**d** the animal implanted with 4T1 cells showing metastatic cancer lesion (**c**; $\times 40$) and presence of bacterial colonies (**d**; $\times 200$), and **e** animal implanted with 4TO7 cells (**c**; $\times 40$). Note that metastatic lesions could be imaged.

Discussion

In this study, we demonstrated that *E. coli* is capable of targeting and proliferating in tumor tissue. Observation of this phenomenon was achieved using a *lux* cassette (*luxCDABE* from *Photobacterium leiognathi* under the control of the *lacZ* promoter), which generated sufficient levels of luciferase-catalyzed light for detection with a cooled CCD camera [17]. The plasmid carrying the *lux* cassette was maintained in the absence of external selection via complementation of an *asd* mutation, which confers a requirement for diaminopimelic acid (DAP); as this is not present in the animal, a loss of the vector leads to bacterial cell death [23, 24].

Although the permeability of vasculature is known to vary from one tumor to the next and also depends upon tumor stage [28], our results indicate that *E. coli* can target a diverse range of tumors, as it accumulated in every type of grafted tumor we tested, including human (SNU-C5) and rodent (CT26, C6, B16F10, ARO, and 4T1) cell lines (Fig. 4). Moreover, we observed that *E. coli* could colonize subcutaneously grafted, small CT26 tumors (<100 mm^3 in size) (Fig. 4a). In addition, although the local environment is known to play an important role in controlling vascular permeability, we detected the accumulation of *E. coli* in an intracecal adenocarcinoma generated in the cecum of nude mice and the subcutaneously grafted CT26 tumors (Fig. 4c). Similarly, we observed that *E. coli* targeted metastases and a primary grafted tumor (Fig. 5). Thus, *E. coli* appears to be capable of targeting a broad range of tumors at different stages.

It should be noted that although the light-generating *E. coli* bacteria were detected initially towards the center of the tumor, as the infection progressed, they appeared to spread to the border between the necrotic and viable areas of the tumor. In the sequential cross-sectional analysis of the tumor mass, we observed strong luciferase-based light emission in the central necrotic region but not at the periphery (Fig. 3b). In subsequent confocal microscopic analysis on tumor tissue obtained from mice infected with *E. coli* pGFP, GFP-expressing bacteria were found in the border region between the peripheral proliferative and central necrotic regions, but were not observed in the peripheral proliferative region of the tumor (Fig. 3d). It is slightly paradoxical to find *E. coli* growing in the hypoxic necrotic center of the tumor, as although it is a facultative anaerobe, it might be expected to grow better in the presence of oxygen. With respect to the accumulation of *E. coli*, bacterial-induced destruction of viable cells might effectively position *E. coli* at the interface with the necrotic region. Furthermore, certain component(s) of *E. coli* (such as lipopolysaccharide) induce tumor cell necrosis; thus, bacteria might migrate chemotactically toward a viable tumor region in search of nutrients.

In this study, we have employed *E. coli* K12 strain, MG1655, which is regarded as the most standard *E. coli* strain with its entire chromosomal DNA sequence available [29]. Traditionally, this strain has been used most widely to understand genetic and physiological bases of *E. coli*. Thus, it should be possible to employ conventional genetic tools and current molecular biological tools to elucidate the mechanism of tumor targeting by bacteria as a whole. In fact, accumulating results suggest that the tumor-targeting phenomenon of bacteria is closely associated with chemotaxis, which is a system employed by bacteria to seek favorable growth condition and to avoid growth adverse condition. We are now currently testing *E. coli* strains carrying various chemotaxis mutations to identify the receptors on bacteria, which would eventually reveal the chemotactic attractant(s) provided by tumor tissues.

In addition, this tumor-targeting capability of bacteria would be extended to a tumor therapy by employing bacteria producing and secreting antitumoral agents. The *E. coli* strain has been traditionally used to produce various proteins owing to the availability of vast knowledge on its gene expression control. Selective protein secretion system of *E. coli* should also provide the means to deliver antitumor protein into tumor tissue. Taken together, the *E. coli* system should be most appropriate to understand the mechanism of tumor-targeting by bacteria and its application to tumor therapy.

Conclusions

In this study, we have demonstrated that genetically-engineered bioluminescent *E. coli* targets a variety of tumor lesions including metastases, enabling noninvasive visualization of both tumors and metastasis. These results are an important improvement upon previous studies using light-emitting bacteria to target tumors, because in our study, metastases and tumors could be noninvasively imaged. Further experiments will involve mechanistic studies of how bacteria selectively target tumors to translate to the clinic [3, 6, 9, 30–32].

Acknowledgements. This study was supported by a grant from the National R&D Program for Cancer Control (0620330-1), Ministry of Health and Welfare, Republic of Korea. H.E.C. was supported by the Korea Science and Engineering Foundation (KOSEF) grant funded by the Korean government (MOST) (No. 2007-04213), J.H.R. by grant no. RTI05-01-01 from the Regional Technology Innovation Program of the Ministry of Commerce, Industry and Energy (MOCIE); and H.S.B. by grant no. RTI-04-03-03 from the Regional Technology Innovation Program of the Ministry of Commerce, Industry and Energy (MOCIE).

References

1. Pawelek JM, Low KB, Bermudes D (2003) Bacteria as tumour-targeting vectors. Lancet Oncol 4:548–556
2. Yu YA, Shabahang S, Timiryasova TM et al. (2004) Visualization of tumors and metastases in live animals with bacteria and vaccinia virus encoding light-emitting proteins. Nat Biotechnol 22:313–320
3. Jain RK, Forbes NS (2001) Can engineered bacteria help control cancer? Proc Natl Acad Sci USA 98:14748–14750
4. Thiele EH, Arison RN, Boxer GE (1964) Oncolysis by Clostridia. III. Effects of Clostridia and chemotherapeutic agents on rodent tumors. Cancer Res 24:222–233
5. Mose JR, Mose G, Propst A, Heppner F (1967) Oncolysis of malignant tumors by Clostridium strain M 55. Med Klin 62:189–193

6. Lemmon MJ, van Zijl P, Fox ME et al. (1997) Anaerobic bacteria as a gene delivery system that is controlled by the tumor microenvironment. Gene Ther 4:791–796
7. Dang LH, Bettegowda C, Huso DL, Kinzler KW, Vogelstein B (2001) Combination bacteriolytic therapy for the treatment of experimental tumors. Proc Natl Acad Sci U S A 98:15155–15160
8. Pawelek JM, Low KB, Bermudes D (1997) Tumor-targeted Salmonella as a novel anticancer vector. Cancer Res 57:4537–4544
9. Zhao M, Yang M, Li XM et al. (2005) Tumor-targeting bacterial therapy with amino acid auxotrophs of GFP-expressing *Salmonella typhimurium*. Proc Natl Acad Sci U S A 102:755–760
10. Zhao M, Yang M, Ma H et al. (2006) Targeted therapy with a *Salmonella typhimurium* leucine–arginine auxotroph cures orthotopic human breast tumors in nude mice. Cancer Res 66:7647–7652
11. Low KB, Ittensohn M, Le T et al. (1999) Lipid A mutant Salmonella with suppressed virulence and TNFalpha induction retain tumor-targeting *in vivo*. Nat Biotechnol 17:37–41
12. Low KB, Ittensohn M, Luo X et al. (2004) Construction of VNP20009: a novel, genetically stable antibiotic-sensitive strain of tumor-targeting Salmonella for parenteral administration in humans. Methods Mol Med 90:47–60
13. Zhao M, Geller J, Ma H, Yang M, Penman S, Hoffman RM (2007) Monotherapy with a tumor-targeting mutant of *Salmonella typhimurium* cures orthotopic metastatic mouse models of human prostate cancer. Proc Natl Acad Sci U S A 104:10170–10174
14. Yu YA, Timiryasova T, Zhang Q, Beltz R, Szalay AA (2003) Optical imaging: bacteria, viruses, and mammalian cells encoding light-emitting proteins reveal the locations of primary tumors and metastases in animals. Anal Bioanal Chem 377:964–972
15. Silhavy TJ, Berman ML, Enquist LW (1984) Experiments with gene fusions. New York: Cold Spring Harbor Laboratory Press
16. Datsenko KA, Wanner BL (2000) One-step inactivation of chromosomal genes in *Escherichia coli* K-12 using PCR products. Proc Natl Acad Sci U S A 97:6640–6645
17. Lee CY, Szittner RB, Meighen EA (1991) The lux genes of the luminous bacterial symbiont, *Photobacterium leiognathi*, of the ponyfish. Nucleotide sequence, difference in gene organization, and high expression in mutant *Escherichia coli*. Eur J Biochem 201:161–167
18. Kang HY, Srinivasan J, Curtiss R 3rd (2002) Immune responses to recombinant pneumococcal PspA antigen delivered by live attenuated *Salmonella enterica serovar typhimurium* vaccine. Infect Immun 70:1739–1749
19. Aslakson CJ, Miller FR (1992) Selective events in the metastatic process defined by analysis of the sequential dissemination of subpopulations of a mouse mammary tumor. Cancer Res 52: 1399–1405
20. Karnes WE Jr, Walsh JH, Wu SV et al. (1992) Autonomous proliferation of colon cancer cells that coexpress transforming growth factor alpha and its receptor. Variable effects of receptor-blocking antibody. Gastroenterology 102:474–485
21. Im SY, Ko HM, Kim JW et al. (1996) Augmentation of tumor metastasis by platelet-activating factor. Cancer Res 56:2662–2665
22. Hoffman RM (1999) Orthotopic metastatic mouse models for anticancer drug discovery and evaluation: a bridge to the clinic. Invest New Drugs 17:343–359
23. Galan JE, Nakayama K, Curtiss R 3rd (1990) Cloning and characterization of the *asd* gene of *Salmonella typhimurium*: use in stable maintenance of recombinant plasmids in Salmonella vaccine strains. Gene 94:29–35
24. Curtiss R III, Nakayama K, Kelly SM (1989) Recombinant avirulent Salmonella vaccine strains with stable maintenance and high level expression of cloned genes *in vivo*. Immunol Invest 18:583–596
25. Baish JW, Jain RK (2000) Fractals and cancer. Cancer Res 60:3683–3688
26. Hobbs SK, Monsky WL, Yuan F et al. (1998) Regulation of transport pathways in tumor vessels: role of tumor type and microenvironment. Proc Natl Acad Sci U S A 95:4607–4612
27. Hashizume H, Baluk P, Morikawa S et al. (2000) Openings between defective endothelial cells explain tumor vessel leakiness. Am J Pathol 156:1363–1380
28. Jain RK (1999) Understanding barriers to drug delivery: high resolution *in vivo* imaging is key. Clin Cancer Res 5:1605–1606
29. Blattner FR, Plunkett G III, Bloch CA et al (1997) The complete genome sequence of *Escherichia coli* K-12. Science 277:1453–1474
30. Sznol M, Lin SL, Bermudes D, Zheng LM, King I (2000) Use of preferentially replicating bacteria for the treatment of cancer. J Clin Invest 105:1027–1030
31. Fox ME, Lemmon MJ, Mauchline ML et al. (1996) Anaerobic bacteria as a delivery system for cancer gene therapy: *in vitro* activation of 5-fluorocytosine by genetically engineered Clostridia. Gene Ther 3:173–178
32. Massoud TF, Gambhir SS (2003) Molecular imaging in living subjects: seeing fundamental biological processes in a new light. Genes Dev 17:545–580